

Probability-based Distance Estimation Model for 3D DV-Hop Localization in WSNs

Penghong Wang, Hao Wang, Wenrui Li, Xiaopeng Fan, *Senior Member, IEEE*, and Debin Zhao, *Member, IEEE*

Abstract—Localization is one of the pivotal issues in wireless sensor network applications. In 3D localization studies, most algorithms focus on enhancing location prediction process, lacking theoretical derivation of the detection distance of an anchor node at the varying hops, which engenders a localization performance bottleneck. To address this issue, we propose a probability-based average distance estimation (PADE) model that utilizes the probability distribution of node distances detected by an anchor node. The aim is to mathematically derive the average distances of nodes detected by an anchor node at different hops. First, we develop a probability-based maximum distance estimation (PMDE) model to calculate the upper bound of the distance detected by an anchor node. Then, we present the PADE model relies on the upper bound obtained of the distance by the PMDE model. Finally, the obtained average distance is used to construct a distance loss function, and it is embedded with the traditional distance loss function into a multi-objective genetic algorithm to predict the locations of unknown nodes. The experimental results demonstrate the proposed method achieves the state-of-the-art performance in both random and multimodal distributed sensor networks. The average localization accuracy is improved by 3.49%-12.66% and 3.99%-22.34%, respectively.

Index Terms—Wireless sensor networks, DV-Hop, probability-based, maximum distance estimation, average distance estimation.

I. INTRODUCTION

WIRELESS sensor networks (WSNs) have shown appealing powers in industry [1]–[3], environmental monitoring [4], healthcare [5], [6], and supply chain management [7]. WSNs are composed mainly of a large number of tiny sensors in an ad-hoc manner. These sensors are deployed in a physical region arbitrarily to monitor and manage environmental conditions in a specific area or to perform certain tasks of collecting information. These tasks typically require obtaining sensor location information, without accurate location information, sharing the data collected by sensors will be inefficient or even infeasible. Global Positioning System (GPS) can provide sensors with the ability to be aware of

This work was supported in part by the National Key Research and Development Program of China (2021YFF0900500), and the National Science Foundation of China (NSFC) under grant U22B2035.

Penghong Wang and Wenrui Li are with the Faculty of Computing, Harbin Institute of Technology, Harbin 150001, China. e-mail: (phwang@hit.edu.cn; 21B903007@stu.hit.edu.cn).

Hao Wang is with the Faculty of Computing, Harbin Institute of Technology, Harbin 150001, China, and also with the College of Engineering, City University of Hong Kong, Kowloon 999077, Hong Kong. e-mail: (ho.wong@cityu.edu.hk).

Xiaopeng Fan and Debin Zhao are with the Faculty of Computing, Harbin Institute of Technology, Harbin 150001, China, and also with the PengCheng Lab, Shenzhen 518055, China. e-mail: (fxp@hit.edu.cn; dbzhao@hit.edu.cn).

Corresponding author: Xiaopeng Fan.

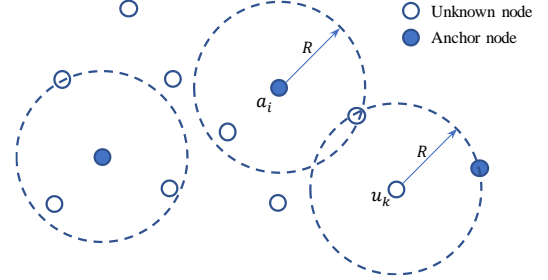


Fig. 1. An example of deploying sensor nodes in a wireless sensor network. a_i : anchor node; u_k : unknown nodes.

location in real-time, but installing GPS on all sensors in a large-scale WSN will significantly increase the cost and energy consumption of the system. In contrast, the range-free localization scheme is well recognized as a promising and low-energy consumption approach for wireless sensor localization.

The range-free localization schemes [8] [9]–[21] [22]–[32] [33]–[42] is one of the prevailing methods in wireless distributed multi-agent localization. Its distinguishing feature lies in its ability to locate without the need for precise measurements of distances or angles between nodes. It can predict the locations of unknown nodes only by relying on the location coordinates of a few nodes and the number of connections between nodes. Fig. 1 shows an example of deploying sensor nodes in a wireless sensor network, including anchor nodes (with known location information) and unknown nodes (with unknown location information). Based on the location of node a_i and the hop counts between nodes, the distance from node u_k to node a_i can be estimated, then the location of node u_k can be predicted. Especially, the distance vector hop (DV-Hop) localization algorithm is one of the most representative range-free localization schemes.

DV-Hop localization algorithm was proposed by Niculescu *et al.* [8] in 2003, and its positioning process contains three parts. **1)** Obtain the minimum connections between nodes based on message passing; **2)** Calculate the Euclidean distance between an unknown node and an anchor node based on the locations of anchor nodes and the minimum connections; **3)** Predict the geographic location of each unknown node based on the information obtained from the above process. The DV-Hop algorithm provides a simple and low-power localization scheme, but its accompanying issue is a large localization error. However, the advantage of its low-cost positioning still attracts scholars to continuously ameliorate the algorithm.

Based on the DV-Hop algorithm, various improved solutions

are proposed to solve wireless sensor localization tasks in two-dimensional (2D) or three-dimensional (3D) spatial scenes. Specifically, most improvement strategies mainly focus on localization issues in 2D planar scenes. For example, some works [9]–[21] focus on providing more accurate solutions for estimating the distance between an unknown node and an anchor node. Especially, [21] provides a distance derivation model for 2D localization scenarios. Others [22]–[32] focus on exploring various location prediction schemes to provide more accurate accuracy for unknown nodes. In recent years, with the deployment and application of wireless sensors in complex terrain such as mountains, underwater, and tunnels, the issue of wireless sensor localization in 3D spatial scenes has gradually attracted attention. Some methods [33]–[42] are proposed to promote positioning performance in 3D spatial scenes, such as connectivity-based and anchor-free [33], distributed algorithms [35] and multi-objective optimization methods [37], [38], [42]. These works primarily focus on enhancing localization algorithms, but lack a theoretical derivation of the detection distance for an anchor node.

In this paper, motivated by [21] for 2D DV-Hop localization, we propose a probability-based maximum distance estimation model and an average distance estimation model for 3D DV-Hop localization. The aim is to explore the correlation among distance estimation, hop counts, and the number of detecting nodes in 3D environments, enhance the overall localization performance. The main contributions are summarized as follows:

- 1) We propose a probability-based maximum distance estimation (PMDE) model to calculate the upper bound of the distance detected by an anchor node. The PMDE model is constructed based on the probability distribution of the distance between each unknown node and an anchor node under different hops.
- 2) Based on the upper bound obtained of the distance by the PMDE model, we propose the probability-based average distance estimation (PADE) model to calculate the average distance detected by an anchor node at different hops.
- 3) We establish a distance loss function based on the obtained expected distance and integrate it with the existing distance loss function into a multi-objective genetic algorithm to accurately predict the location of each unknown node. The numerical results demonstrate significant gains of our approach compared to the state-of-the-art techniques.

The rest of the paper is organized as follows: Section II reviews the improved DV-Hop algorithm in 3D localization scenarios. Section III proposes a probability-based maximum distance estimation model. Section IV proposes a probability-based average distance estimation model. Section V constructs two distance loss functions and embeds them into the multi-objective optimization algorithm. Section VI discusses the simulation results. Finally, the conclusion of this paper is summarized.

II. RELATED WORK

A. 3D DV-Hop

The 3D DV-Hop algorithm is conceptually akin to its 2D counterpart. Firstly, the average hop distance for each anchor node is determined based on the minimum hops obtained through the flooding process of the anchor nodes, and it is calculated by

$$A_Dis_i = \frac{\sum_j \sqrt{(x_i - x_j)^2 + (y_i - y_j)^2 + (z_i - z_j)^2}}{\sum_j Hop_{i,j}}, \quad (1)$$

where (x_i, y_i, z_i) and (x_j, y_j, z_j) indicate the coordinates of a_i and a_j , respectively, and $Hop_{i,j}$ indicates the minimum connections between a_j and a_i . The estimated distance between u_k and a_i is calculated by

$$Dis_{i,k} = A_Dis_i \cdot Hop_{i,k}, \quad (2)$$

where $Hop_{i,k}$ stands for the minimum connections between u_k and a_i . Finally, the location of each u_k can be predicted by the least mean square estimator.

B. 3D DV-Hop-based Improved Schemes

In 2D positioning scenarios, the distance estimation strategies [13], [16], [21] and the position optimization strategies [23], [24], [27] have significantly advanced the progress of localization technologies. However, in real-world applications, when sensors are deployed in areas with varying terrain and elevation, the positioning system must be able to accurately determine the vertical and horizontal locations of nodes. In this case, it is necessary to develop 3D positioning methods to effectively overcome the limitations of 2D positioning methods in the vertical dimension. [33] proposes a connectivity-based and anchor-free localization scheme, aiming to address the challenge of node localization in large-scale 2D/3D sensor networks with concave areas. This method can achieve smooth expansion from 2D to 3D. [35] proposes a distributed algorithm to achieve accurate 3D sensor localization. Specifically, the proposed scheme utilizes connected information to implement an approximate convex partitioning technique that divides the entire network into multiple subnetworks. Subsequently, the multidimensional scaling-based algorithm is employed to precisely locate nodes within each subnetwork. [37] constructs a distance loss function based on the average distance detected per hop of all anchor nodes and employs a multi-objective localization scheme to optimize the predicted node positions. This work is the first to apply multi-objective optimization algorithms to 3D positioning problem. [38] develops a localization scheme using multi-objective particle swarm optimization. It further enhances the application of multi-objective optimization algorithms in 3D sensor localization problems. [41] presents a maximum similarity path method for estimating the distance between an unknown node and an anchor node and utilizes the cosine theorem to correct the estimated distance. Additionally, an improved water flow optimizer is employed to predict the locations of the unknown nodes.

These works primarily focus on enhancing localization algorithms, but lack a theoretical derivation of the detection distance for an anchor node. In this work, we propose a probability-based maximum distance estimation model and an average distance estimation model for 3D DV-Hop localization, which extends the distance estimation model from 2D localization scenes in [21] to 3D localization scenes.

III. PROBABILITY-BASED MAXIMUM DISTANCE ESTIMATION

Our goal is to estimate the average distance detected by an anchor node at different hops for locating each unknown node position. However, the computation of the average distance requires obtaining the upper bound of the distance detected by an anchor node. To address this issue, we propose a probability-based maximum distance estimation model for 3D sensor localization scenarios in this section. Its aim is to provide accurate distance estimation for the outermost detection node that is detected by anchor nodes at different hop counts. Fig. 2 provides a visualization example that represents the information transmission process of sensor nodes.

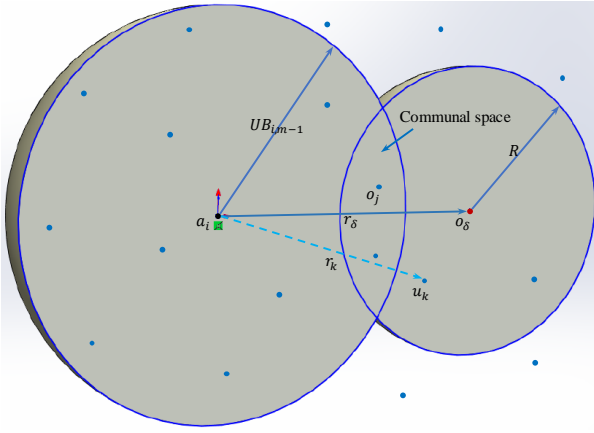


Fig. 2. The example of multi hop information transmission for sensors. a_i : an anchor node, u_k : an unknown node, o_j and o_δ : an ordinary (anchor or unknown) node, r_δ : the distance between o_δ and a_i , $UB_{i,m-1}$: the expected distance of the outermost node detected by node a_i when $hop = m - 1$.

Assuming that the deployment of sensor nodes in 3D space follows a uniform distribution, as shown in Fig. 2. a_i is an anchor node, o_j and o_δ are ordinary nodes (anchor or unknown nodes), r_δ indicates the distance between o_δ and a_i , and $UB_{i,m-1}$ is the distance of the outermost node detected by a_i when $hop = m - 1$. In Fig. 2, let o_δ be the outermost node detected by a_i when $hop = m$. In this case, two conditions need to be satisfied: **1)** o_δ is the outermost node within the detection range of a_i when $hop = m$; **2)** the communal space contains at least one node relay node (denoted as o_j). Based on the above analysis, let $P_{i,m-1}(o_j)$ represent the probability that there exists at least one o_j in the communal space, let $P_{i,m}(o_\delta)$ represent the probability that o_δ is the outermost node within the detection range of a_i when $hop = m$. The probability density ($P_{i,m}^{true}(o_\delta)$) of the outermost node that a_i can detect when $hop = m$ is calculated by

$$P_{i,m}^{true}(o_\delta) = P_{i,m-1}(o_j)P_{i,m}(o_\delta). \quad (3)$$

Next, we introduce the calculation methods of $P_{i,m-1}(o_j)$ and $P_{i,m}(o_\delta)$ involved in (3). Significantly, when $m = 1$, the distribution of nodes is shown in Fig. 3. Let o_δ represent the outermost node detected by a_i when $m = 1$, the probability $P_{i,m}(o_\delta)$ is calculated by

$$\begin{aligned} P_{i,1}(o_\delta) &= \prod_{k=1}^{n_{i,1}} P_{i,1}(r_\delta \geq r_k) \\ &= \prod_{k=1}^{n_{i,1}} \frac{\int_0^{r_\delta} (R^2 - r^2) dr}{\int_0^R (R^2 - r^2) dr}, m = 1, \quad (4) \\ &= \left(\frac{r_\delta^3}{R^3} \right)^{n_{i,1}} \end{aligned}$$

where r_δ represents the distance between o_δ and a_i , and $r_\delta = \max(r_1, r_2, \dots, r_k, \dots, r_{n_1})$, $n_{i,1}$ represents the number of nodes detected by a_i when $hop = 1$. In this scenario, the nodes detected by a_i are independent of any relay nodes, i.e., $P_{i,m-1}(o_j) = 1$, and (3) can be simplified as $P_{i,1}^{true}(o_\delta) = P_{i,1}(o_\delta)$.

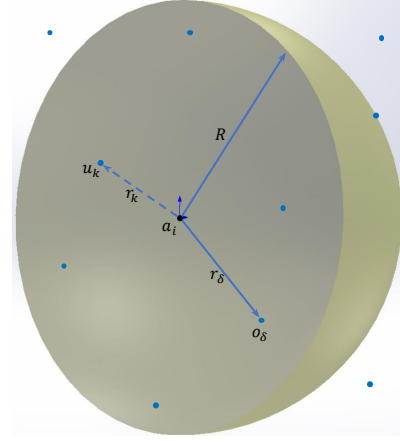


Fig. 3. The example of node distribution detected by a_i when $m = 1$.

When $m > 1$, we model the distribution of nodes and the multi-hop transmission characteristics of information in a Cartesian coordinate system, as depicted in Fig. 4. In Fig. 4 (a), a_i denotes the center of the Cartesian coordinate system, o_δ denotes the outermost node detected by a_i when $hop = m$, its coordinates are $(r_\delta, 0)$. o_j is Located at the center of the communal space, with coordinates $(r_j, 0)$. The coordinates of nodes b and c are $(r_\delta - R, 0)$ and $(UB_{i,m-1}, 0)$, respectively. Fig. 4 (b) provides a detailed illustration of the space S_1 in Fig. 4 (a). The probability $P_{i,m}(o_\delta)$ is calculated by

$$\begin{aligned} P_{i,m}(o_\delta) &= \prod_{k=1}^{n_{i,m}} P_{i,m}(r_\delta \geq r_k) \\ &= \prod_{k=1}^{n_{i,m}} \frac{\int_0^{r_\delta} (R^2 - r^2) dr}{\int_0^{m \cdot R} (R^2 - r^2) dr}, m > 1, \quad (5) \\ &= \left(\frac{r_\delta^3}{(m \cdot R)^3} \right)^{n_{i,m}} \end{aligned}$$

where $r_\delta = \max(r_1, r_2, \dots, r_k, \dots, r_{n_m})$, $n_{i,m}$ denotes the number of nodes detected by a_i when $hop \leq m$.

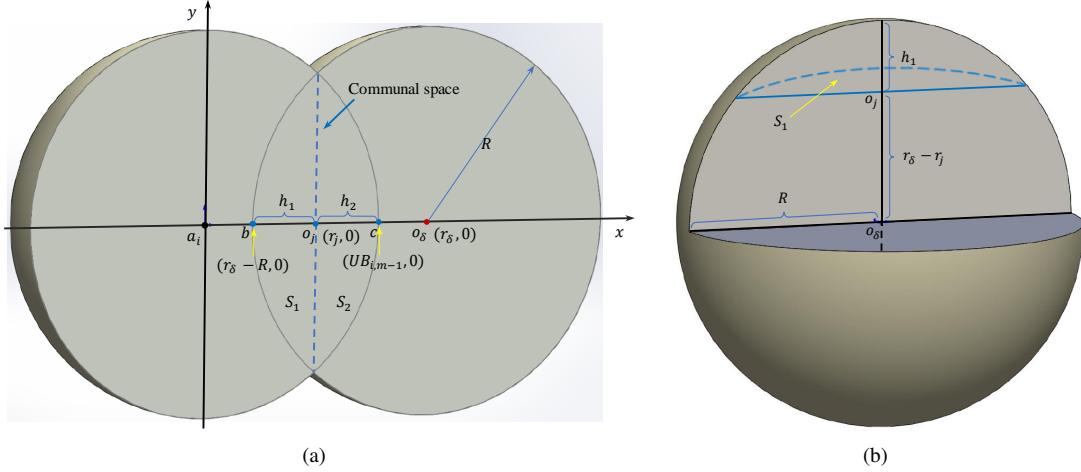


Fig. 4. An example of outermost detection node analysis. a_i : an anchor node, o_δ : an ordinary node, S_1 and S_2 : a part of the communal space, R : communication radius, $UB_{i,m-1}$: the expected distance of the outermost node detected by node a_i when $hop = m - 1$.

Correspondingly, $P_{i,m-1}(o_j)$ is calculated by

$$P_{i,m-1}(o_j) = 1 - \left(1 - \frac{CS}{S_{i,m-1}}\right)^\epsilon, \quad (6)$$

where ϵ indicates the node density, and it is calculated by $\epsilon = \frac{n_{i,m-1} - n_{i,m-2}}{2}$. $S_{i,m-1}$ denotes the maximum space detected by a_i when $hop = m - 1$, it is calculated by

$$S_{i,m-1} = \frac{4}{3}\pi UB_{i,m-1}^3, \quad (7)$$

and CS denotes the communal space detected by a_i and o_δ , it is composed of S_1 and S_2 . Based on the analysis of Fig. 4, CS is calculated by

$$CS = \int_{r_\delta - R}^{r_j} \pi(R^2 - x^2)dx + \int_{r_j}^{E_{i,m-1}(o_\delta)} \pi(UB_{i,m-1}^2 - x^2)dx, \quad (8)$$

where $UB_{i,m-1}$ denotes the expected distance of the outermost node detected by a_i when $hop = m - 1$. $UB_{i,m}$ is calculated by

$$UB_{i,m} = \int_0^{m \cdot R} r_\delta P_{i,m}^{true}(o_\delta)' dr_\delta. \quad (9)$$

Specially, when $m = 1$, its expected distance is $\frac{3n_{i,1}}{3n_{i,1}+1}R$. This result indicates that when the number of detected nodes $n_1 \rightarrow \infty$, the $UB_{i,1} = R$. It verifies the reliability of our model.

IV. PROBABILITY-BASED AVERAGE DISTANCE ESTIMATION

In this section, based on the upper boundary obtained from the previous section, we propose a probability-based average distance estimation model for 3D sensor localization scenarios. Compared to DEM-DV-Hop [21], the PADE model considers the conditional probability during node detection when calculating the average distance. This consideration can enable the PADE model to achieve higher accuracy in distance

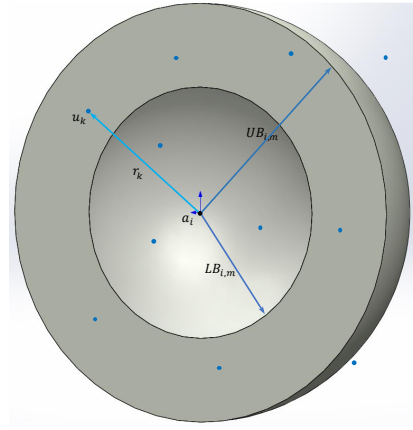


Fig. 5. An example of the distribution space of u_k when $m = 1$. r_k : the distance between u_k and a_i , $UB_{i,m}$ and $LB_{i,m}$: the upper and lower bounds of r_k .

estimation. Based on the information presented in Fig. 2 and the PMDE model, we present the derivation process of the PADE model. Similarly, two conditions need to be satisfied: **1)** u_k is a node within the detection range of a_i when $hop = m$; **2)** o_j is a relay node located in the communal space.

Specifically, let $P_{i,m-1}(o_j)$ represent the probability that there exists at least one o_j in the communal space; let $P_{i,m}(u_k)$ represent the probability that u_k is an unknown node within the detection range of a_i when $hop = m$. Let $P_{i,m}^{true}(u_k)$ represent the probability density that u_k can be detected by a_i when $hop = m$. and $P_{i,m}^{true}(u_k)$ is calculated by

$$P_{i,m}^{true}(u_k) = P_{i,m-1}(o_j)P_{i,m}(u_k), \quad (10)$$

where $P_{i,m-1}(o_j)$ is calculated by (6).

The distribution of u_k is shown in Fig. 5. In this figure, r_k denotes the distance between u_k and a_i , $UB_{i,m}$ and $LB_{i,m}$ denote the upper and lower bounds of r_k . $P_{i,m}(u_k)$ can be considered as the probability density function of u_k within a

Algorithm 1 Multi-objective 3D localization genetic algorithm.

Input: The locations of anchor nodes and the ground truth locations of unknown nodes

Output: The predicted locations of unknown nodes

- 1: Initialize parameters with Table I and initial population
- 2: Statistical $hop_{i,k}$ and $n_{i,m}$ based on DV-Hop algorithm
- 3: $Dis_{i,k} \leftarrow (2)$
- 4: $UB_{i,m} \leftarrow (9)$
- 5: $E_dis_{i,k} \leftarrow (12)$
- 6: **for** $iter = 1 \rightarrow M_Iter$ **do**
- 7: Perform crossover and mutation operations based on Pc and Pm .
- 8: $\mathcal{L}_1 \leftarrow (13)$
- 9: $\mathcal{L}_2 \leftarrow (14)$.
- 10: Calculate non-dominated sorting and crowding distance based on the values of \mathcal{L}_1 and \mathcal{L}_2 .
- 11: Select competitive population individuals based on sorting results.
- 12: **end**

circular spatial domain, and it is calculated by

$$P_{i,m}(u_k) = \frac{r_k^3 - LB_{i,m}^3}{UB_{i,m}^3 - LB_{i,m}^3}, \quad (11)$$

where $UB_{i,m}$ is calculated by (9), Inspired by [16] and [21], when $m > 2$, we define the expected distance ($E_dis_{i,m}$) of u_k detected by a_i at $hop = m - 1$ as $LB_{i,m}$. The $E_dis_{i,m}$ is calculated by

$$E_dis_{i,m} = \int_{LB_{i,m}}^{UB_{i,m}} r_k P_{i,m}^{true}(u_k)' dr_k, \quad (12)$$

where $LB_{i,m} = E_dis_{i,m-1}$. When $m = 2$, the value of $LB_{i,m}$ is equal to $UB_{i,1}$. Specially, when $m = 1$, the value of $LB_{i,m}$ is equal to 0, the result of $E_dis_{i,m}$ is $\frac{3}{4}UB_{i,1}$.

It should be emphasized that the calculation method described in (12) differs entirely from the approaches outlined in [16] and [21]. In this work, we specifically calculate nodes that fulfill the specified conditions within the defined search space. In contrast, [16] and [21] calculate all nodes within the defined search space. It suggests that our approach has the potential to theoretically offer more precise accuracy in distance estimation.

V. MULTI-OBJECTIVE OPTIMIZATION

In this section, we construct two distance loss functions (\mathcal{L}_1 and \mathcal{L}_2) based on $Dis_{i,k}$ and $E_dis_{i,k}$ derived from the aforementioned analysis. These distance loss functions are subsequently integrated into multi-objective genetic algorithms [43] to predict the location of u_k . This scheme endeavors to deliver precise location prediction solutions for unknown nodes.

Based on the $Dis_{i,k}$ obtained from (2), we can construct the first distance loss function (\mathcal{L}_1) as follows

$$\min \mathcal{L}_1(x_k, y_k, z_k) = \sum_{i=1}^{N_a} (\sqrt{(x_i - x_k)^2 + (y_i - y_k)^2 + (z_i - z_k)^2} - Dis_{i,k})^2, \quad (13)$$

where (x_i, y_i, z_i) and (x_k, y_k, z_k) refer to the locations of a_i and u_k , respectively. Similarly, Based on the $E_dis_{i,k}$ obtained from (12), we can construct the second distance loss function (\mathcal{L}_2) as follows

$$\min \mathcal{L}_2(x_k, y_k, z_k) = \sum_{i=1}^{N_a} (\sqrt{(x_i - x_k)^2 + (y_i - y_k)^2 + (z_i - z_k)^2} - E_dis_{i,k})^2, \quad (14)$$

Algorithm 1 provides pseudo-code for a multi-objective 3D localization genetic algorithm. Where $hop_{i,k}$ denotes the hop count between u_k and a_i , $n_{i,m}$ denotes the number of nodes detected by a_i when $hop \leq m$. It should be emphasized that the key innovation and contribution of this paper is the proposal of the PADE model and the PMDE model. The purpose is to provide a solid theoretical foundation for algorithms and enhance the overall localization performance. Therefore, for multi-objective genetic algorithms, we follow the original design scheme. The details of crossover, mutation, selection, and non-dominated sorting operation involved in Algorithm 1 can be found in [43].

VI. SIMULATION AND ANALYSIS

A. Experimental Setup

Datasets. Following [37], we chose a randomly distributed network to evaluate localization performance. Moreover, considering the potential deployment of sensors in mountainous environments during real applications, we chose a multimodal distributed sensor network for evaluating the performance. The aim is to assess the generalization ability of the proposed model in adapting to complex deployment environments in practical scenarios. Each sensor network contains the locations of 150 sensor nodes distributed in a 3D space (100m×100m×100m), as shown in Fig. 6. A subset of the node locations corresponds to the locations of anchor nodes, while another subset corresponds to the ground truth (gt) locations of unknown nodes, corresponding to \star and \bullet in Fig. 6, respectively.

TABLE I
SIMULATION PARAMETERS.

Parameters	Value	Parameters	Value
Pc	0.9	N_a	10-35
Pm	0.1	N_u	115-140
Ps	20	R	25-40
Independent repeat test	50	M_Iter	500

Pc : crossover probability, Pm : mutation probability, Ps : Population size, N_u : the number of unknown nodes, M_Iter : maximum iterations, independent repeat test: the number of independent experiments; population size: the number of individuals in the population.

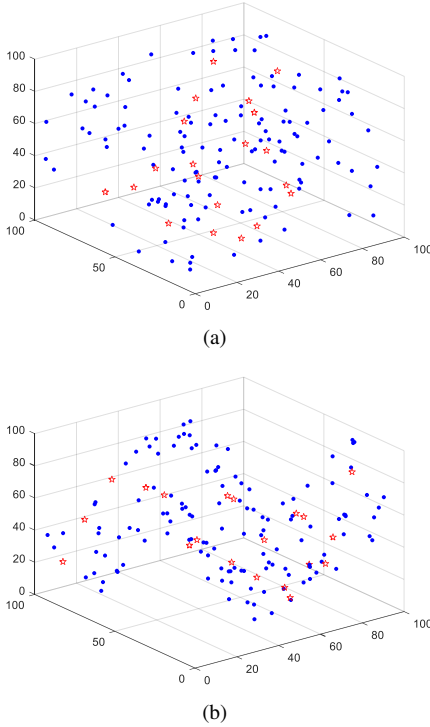


Fig. 6. Two different distribution test datasets. (a): random distributed sensor network; (b): multimodal distributed sensor network. \star : anchor node, \bullet : unknown node.

Parameters. The detailed experimental parameters of the algorithm are listed in Table I.

Performance Metric. In this work, we provide multiple metrics to comprehensively evaluate the effectiveness of the proposed method. Firstly, we employ the normalized average localization errors (*ALEs*) as a metric to assess the algorithm's localization errors in various testing scenarios. This metric aims to evaluate the generalization capability of the proposed algorithm. The *ALEs* are calculated by

$$ALEs = \frac{100\%}{N_u R} \sum_{k=1}^{N_u} \sqrt{(x_k^{gt} - x_k)^2 + (y_k^{gt} - y_k)^2 + (z_k^{gt} - z_k)^2}, \quad (15)$$

where (x_k, y_k, z_k) and $(x_k^{gt}, y_k^{gt}, z_k^{gt})$ represent the prediction coordinates and ground truth coordinates of an u_k respectively. Next, the average performance gain (*APG*) is used to evaluate the comprehensive localization gain of the proposed algorithm compared to other algorithms. This metric focuses on evaluating the effectiveness of the proposed algorithm. The *APG* is calculated by

$$APG = \text{mean} \sum (ALEs_{other} - ALEs_{our}), \quad (16)$$

where $ALEs_{other}$ represents the *ALEs* of other algorithms used for comparison in this paper. Lastly, we employ the 95% confidence interval of *ALEs* (*ALEs* follow a Gaussian distribution) as a mean to visualize the distribution of errors. This metric aims to evaluate the stability of the proposed algorithm. The confidence interval is calculated by

$$[\bar{X} - \frac{S}{\sqrt{n}} t_{\frac{\alpha}{2}}(n-1), \bar{X} + \frac{S}{\sqrt{n}} t_{\frac{\alpha}{2}}(n-1)], \quad (17)$$

where \bar{X} , S^2 , n , and α denote the mean, variance, and samples size, and significance level, respectively. In this work, $\bar{X} = \frac{1}{n} \sum_i^n ALE_i$, $S^2 = \frac{\sum_i^n (ALE_i - \bar{X})^2}{n-1}$, $n = 50$, and $\alpha = 0.05$.

B. Comparison with State-of-the-art Results

To objectively showcase the effectiveness and stability of the proposed method, we compare several baseline algorithms. Specifically, DV-Hop 3D [8] is a classic range-free localization algorithm. DEM-DV-Hop 3D [21] is an algorithm that uses distance estimation strategy and represents the state-of-the-art in 2D positioning scenes. OCS-DV-Hop 3D [23] and IAGA-DV-Hop 3D [27] are algorithms based on enhanced cuckoo search and genetic algorithm for position prediction, respectively. CC-DV-Hop 3D [24] is a classic method for transforming the localization problem into constrained optimization problem. NSGAI-DV-Hop 3D [37] is a classic multi-objective localization scheme in 3D positioning scenes.

Table II and Table III provide performance comparisons with current excellent works under random distributed sensor network and a multimodal distributed sensor network, respectively. In general, the *ALEs* of the proposed method demonstrate a consistent trend across various test datasets, whereby the *ALEs* decrease as the number of anchor nodes increases. Meanwhile, the *ALEs* decrease with the increase of node communication radius. In addition, the results demonstrate that the *ALEs* of the proposed method outperforms DV-Hop 3D [8], DEM-DV-Hop 3D [21], IAGA-DV-Hop 3D [27], and NSGAI-DV-Hop 3D [37] across all test conditions. When $N_a = 10$, the *ALEs* of the proposed method is more outstanding than OCS-DV-Hop 3D [23] and CC-DV-Hop 3D [24]; when $N_a > 10$, the *ALEs* of the proposed method is superior to these two algorithms across almost all conditions. In summary, based on the results presented in Tables II and III, it is evident that the proposed method has achieved significant gains compared to the comparative algorithm.

Table IV displays the average localization accuracy (*ALA*, $ALA = 1 - \text{mean}(ALEs)$) of the algorithm and the *APG* achieved by the proposed method in comparison to other algorithms across two different test data. The results indicate that the proposed method achieves an *ALA* of 63.30% and 58.09% in random and multimodal distributed sensor networks, respectively. Compared to the state-of-the-art algorithms, the proposed method achieves *APG* ranging from 3.49% to 12.66% in the random distributed sensor network and from 3.99% to 22.34% in the multimodal distributed sensor network. It is noteworthy that in 2D localization scenarios, [21] achieves the best localization performance in comparison algorithms. However, in 3D localization scenarios, its comprehensive localization performance is inferior to algorithms such as [23], [24], and [27]. This phenomenon highlights the infeasibility of transferring probability-based distance estimation models from 2D environments to their 3D counterparts without appropriate modifications. It demonstrates the significance of this work.

Fig. 7 provides a visualization of the 95% confidence interval (CI) for the *ALEs* samples, considering the parameters $N_a = 25$ and $R = 40$. In this study, a consistent confidence level and sample size were maintained throughout the testing

TABLE II
THE ALEs IN THE RANDOMLY TOPOLOGICAL NETWORKS.

N_a	10				15				20				
	R (m)	25	30	35	40	25	30	35	40	25	30	35	40
DV-Hop 3D [8]	90.06	62.68	49.15	47.56	74.71	53.59	41.10	35.59	65.52	49.83	36.02	34.60	
OCS-DV-Hop 3D [23]	65.38	46.74	37.66	35.16	61.47	40.29	32.50	32.92	60.38	39.12	31.83	30.06	
NSGAI-DV-Hop 3D [37]	94.62	62.79	52.77	47.56	78.98	51.37	38.71	35.25	71.40	44.59	34.14	29.71	
CC-DV-Hop 3D [24]	73.60	42.11	35.84	34.54	69.46	44.31	30.85	29.68	60.58	37.88	30.39	28.67	
IAGA-DV-Hop 3D [27]	89.12	56.82	47.18	43.62	69.27	45.85	34.12	30.69	64.69	40.12	30.29	25.86	
DEM-DV-Hop 3D [21]	102.22	63.76	51.10	45.48	78.51	50.01	38.30	32.09	73.68	46.12	33.01	27.32	
Proposed method	84.11	50.27	41.54	38.49	62.51	39.88	30.50	27.33	57.88	35.08	27.85	23.62	

N_a	25				30				35				
	R (m)	25	30	35	40	25	30	35	40	25	30	35	40
DV-Hop 3D [8]	74.56	48.98	36.60	34.49	72.73	43.13	31.92	31.72	63.54	41.38	32.93	32.21	
OCS-DV-Hop 3D [23]	58.08	39.97	29.93	28.66	61.93	38.92	29.67	27.47	60.28	39.29	28.96	28.50	
NSGAI-DV-Hop 3D [37]	62.41	40.47	30.29	26.90	57.62	36.19	27.28	23.67	55.52	35.25	26.37	23.42	
CC-DV-Hop 3D [24]	61.50	35.78	29.65	29.24	56.26	36.13	27.83	26.27	53.71	35.10	28.01	27.26	
IAGA-DV-Hop 3D [27]	57.12	36.78	26.38	23.83	53.33	32.79	23.99	21.12	51.09	31.83	23.04	20.61	
DEM-DV-Hop 3D [21]	65.12	41.95	29.47	25.17	60.97	37.73	26.79	22.99	57.22	36.85	26.20	22.26	
Proposed method	50.04	32.71	24.78	21.57	46.25	29.85	22.33	19.18	44.99	29.56	21.82	18.73	

TABLE III
THE ALEs IN THE MULTIMODEL DISTRIBUTED NETWORK.

N_a	10				15				20				
	R (m)	25	30	35	40	25	30	35	40	25	30	35	40
DV-Hop 3D [8]	98.61	81.91	81.91	65.69	79.74	73.45	57.05	53.29	80.54	65.92	52.02	55.46	
OCS-DV-Hop 3D [23]	70.78	63.10	68.47	56.61	58.57	51.61	43.17	46.70	45.66	42.72	37.00	33.32	
NSGAI-DV-Hop 3D [37]	96.45	79.63	75.50	64.23	71.29	62.92	52.35	50.55	58.42	51.34	42.42	41.39	
CC-DV-Hop 3D [24]	76.18	67.89	58.34	49.77	71.13	68.31	49.17	48.59	67.27	58.49	45.31	47.73	
IAGA-DV-Hop 3D [27]	86.78	77.54	68.64	56.70	62.34	58.04	45.45	45.57	48.95	45.43	36.01	35.07	
DEM-DV-Hop 3D [21]	93.03	80.01	72.59	59.06	71.98	64.02	50.32	48.43	57.83	50.76	40.58	38.17	
Proposed method	76.91	71.44	64.58	53.69	55.91	52.01	42.48	41.29	42.24	38.65	32.86	32.03	

N_a	25				30				35				
	R (m)	25	30	35	40	25	30	35	40	25	30	35	40
DV-Hop 3D [8]	75.53	64.26	49.22	52.10	72.41	61.88	51.56	52.24	66.65	55.12	49.45	46.05	
OCS-DV-Hop 3D [23]	45.48	43.85	37.69	35.55	47.69	39.44	36.20	33.76	50.34	41.74	37.87	34.37	
NSGAI-DV-Hop 3D [37]	54.40	47.99	40.79	40.07	51.17	45.61	38.86	38.03	50.63	45.21	38.92	38.08	
CC-DV-Hop 3D [24]	59.67	51.77	39.88	41.80	53.73	49.13	42.23	38.42	51.50	44.99	39.74	37.84	
IAGA-DV-Hop 3D [27]	45.41	41.23	34.40	33.33	45.03	39.66	33.63	32.00	43.89	38.82	33.36	31.43	
DEM-DV-Hop 3D [21]	51.82	46.43	37.98	36.02	49.48	44.61	36.80	34.11	48.41	43.95	36.70	33.90	
Proposed method	39.09	36.13	32.38	31.06	37.08	34.16	31.63	29.42	36.77	33.40	31.72	28.99	

TABLE IV
COMPARISON OF COMPREHENSIVE LOCALIZATION PERFORMANCE.

Node distribution type	Random		Multimodal	
	ALa	APG	ALa	APG
Algorithms				
DV-Hop 3D [8]	50.64	12.66 ↑	35.75	22.34 ↑
OCS-DV-Hop 3D [23]	58.95	4.35 ↑	54.10	3.99 ↑
NSGAI-DV-Hop 3D [37]	54.70	8.60 ↑	46.82	11.27 ↑
CC-DV-Hop 3D [24]	59.81	3.49 ↑	47.55	10.54 ↑
IAGA-DV-Hop 3D [27]	59.19	4.11 ↑	53.39	4.70 ↑
DEM-DV-Hop 3D [21]	54.40	8.9 ↑	48.87	9.22 ↑
Proposed method	63.30	0.00	58.09	0.00

process. As a result, the width of the CI accurately reflects the dispersion level of samples. The results demonstrate that the CI width of the proposed method is slightly wider than

OCS-DV-Hop 3D [23], but the localization performance is significantly better than OCS-DV-Hop 3D [23]. In addition, the CI width of the proposed method is significantly better than other comparative algorithms. The results of CI indicate that the proposed method demonstrates favorable stability and reliability. The predicted location of each node obtained by DV-Hop 3D [8] and CC-DV-Hop 3D [24] is unique and thus not considered in the comparison of the CI.

VII. CONCLUSIONS

In 3D localization studies, most algorithms focus on enhancing position estimation algorithms, lacking theoretical derivation of the detection distance of an anchor node at the varying hops, which engenders a localization performance bottleneck. To address this issue, we propose a PADE model for 3D

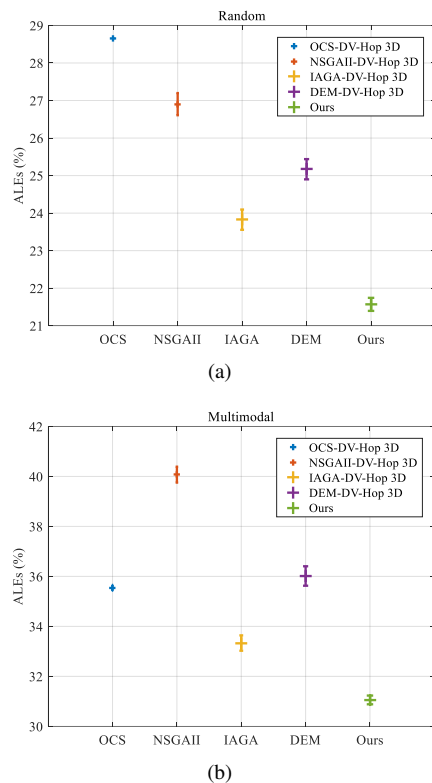


Fig. 7. The 95% confidence interval for $ALEs$ samples. (a): random distributed sensor networks; (b): Multimodal distributed sensor networks. $N_a = 25$ and $R = 40$.

DV-Hop localization in WSNs. The aim is to mathematically derive the average distances of nodes detected by an anchor node at different hops. First, we develop a probability-based maximum distance estimation (PMDE) model to calculate the upper bound of the distance detected by an anchor node. Then, we present the PADE model relies on the upper bound obtained of the distance by the PMDE model. Finally, the obtained average distance is used to construct a distance loss function, and it is embedded with the traditional distance loss function into a multi-objective genetic algorithm to predict the locations of unknown nodes. The experimental results demonstrate the proposed method achieves the state-of-the-art performance in both random and multimodal distributed sensor networks.

In future work, we will investigate obstacle detours in 3D positioning scenarios and apply the derived method to diverse complex deployment environments.

REFERENCES

- [1] A. Tiwari, P. Ballal, and F. L. Lewis, "Energy-efficient wireless sensor network design and implementation for condition-based maintenance," *ACM Transactions on Sensor Networks*, vol. 3, no. 1, pp. 1–es, 2007.
- [2] V. J. Hodge, S. O'Keefe, M. Weeks, and A. Moulds, "Wireless sensor networks for condition monitoring in the railway industry: A survey," *IEEE Transactions on Intelligent Transportation Systems*, vol. 16, no. 3, pp. 1088–1106, 2015.
- [3] G. Kaur, P. Chanak, and M. Bhattacharya, "Obstacle-aware intelligent fault detection scheme for industrial wireless sensor networks," *IEEE Transactions on Industrial Informatics*, vol. 18, no. 10, pp. 6876–6886, 2022.

- [4] A. Boubrima, W. Bechkit, and H. Rivano, "Optimal wsn deployment models for air pollution monitoring," *IEEE Transactions on Wireless Communications*, vol. 16, no. 5, pp. 2723–2735, 2017.
- [5] E. M. Ar-Reyouchi, K. Ghomid, D. Ar-Reyouchi, S. Rattal, R. Yahiaoui, and O. Elmazria, "Protocol wireless medical sensor networks in iot for the efficiency of healthcare," *IEEE Internet of Things Journal*, vol. 9, no. 13, pp. 10 693–10 704, 2022.
- [6] F. Zhu, X. Yi, A. Abuadba, I. Khalil, S. Nepal, X. Huang, and X. Yan, "Certificate-based anonymous authentication with efficient aggregation for wireless medical sensor networks," *IEEE Internet of Things Journal*, vol. 9, no. 14, pp. 12 209–12 218, 2022.
- [7] J. Wang, H. Wang, J. He, L. Li, M. Shen, X. Tan, H. Min, and L. Zheng, "Wireless sensor network for real-time perishable food supply chain management," *Computers and Electronics in Agriculture*, vol. 110, pp. 196–207, 2015.
- [8] D. Niculescu and B. Nath, "Dv based positioning in ad hoc networks," *Telecommunication Systems*, vol. 22, no. 1, pp. 267–280, 2003.
- [9] Y. Wang, X. Wang, D. Wang, and D. P. Agrawal, "Range-free localization using expected hop progress in wireless sensor networks," *IEEE Transactions on Parallel and Distributed Systems*, vol. 20, no. 10, pp. 1540–1552, 2009.
- [10] B. Xiao, L. Chen, Q. Xiao, and M. Li, "Reliable anchor-based sensor localization in irregular areas," *IEEE Transactions on Mobile Computing*, vol. 9, no. 1, pp. 60–72, 2010.
- [11] G. Wu, S. Wang, B. Wang, Y. Dong, and S. Yan, "A novel range-free localization based on regulated neighborhood distance for wireless ad hoc and sensor networks," *Computer Networks*, vol. 56, no. 16, pp. 3581–3593, 2012.
- [12] S. Zaidi, A. El Assaf, S. Affes, and N. Kandil, "Accurate range-free localization in multi-hop wireless sensor networks," *IEEE Transactions on Communications*, vol. 64, no. 9, pp. 3886–3900, 2016.
- [13] L. Cui, C. Xu, G. Li, Z. Ming, Y. Feng, and N. Lu, "A high accurate localization algorithm with dv-hop and differential evolution for wireless sensor network," *Applied Soft Computing*, vol. 68, pp. 39–52, 2018.
- [14] P. Wang, L. Du, Z. Cui, X. Cai, and L. Xie, "A multi-objective localization algorithm with real average distance in wsn," in *2019 IEEE 21st International Conference on High Performance Computing and Communications; IEEE 17th International Conference on Smart City; IEEE 5th International Conference on Data Science and Systems (HPCC/SmartCity/DSS)*, 2019, pp. 29–36.
- [15] G. Liu, Z. Qian, and X. Wang, "An improved dv-hop localization algorithm based on hop distances correction," *China Communications*, vol. 16, no. 6, pp. 200–214, 2019.
- [16] X. Cai, P. Wang, Z. Cui, W. Zhang, and J. Chen, "Weight convergence analysis of dv-hop localization algorithm with ga," *Soft Computing*, vol. 24, no. 23, pp. 18 249–18 258, 2020.
- [17] K. Chen, C. Wang, L. Chen, X. Niu, Y. Zhang, and J. Wan, "Smart safety early warning system of coal mine production based on wsn," *Safety science*, vol. 124, p. 104609, 2020.
- [18] X. Liu, F. Han, W. Ji, Y. Liu, and Y. Xie, "A novel range-free localization scheme based on anchor pairs condition decision in wireless sensor networks," *IEEE Transactions on Communications*, vol. 68, no. 12, pp. 7882–7895, 2020.
- [19] P. Wang, X. Cai, and L. Xie, "A modified error-oriented weight positioning model based on dv-hop," *KSII Transaction on Internet and Information Systems*, vol. 16, no. 2, pp. 405–423, 2022.
- [20] T. Chen, S. Hou, and L. Sun, "An enhanced dv-hop positioning scheme based on spring model and reliable beacon node set," *Computer Networks*, vol. 209, p. 108926, 2022.
- [21] P. Wang, R. Zhou, X. Fan, and D. Zhao, "A distance estimation model for dv-hop localization in wsn," *IEEE Transactions on Vehicular Technology*, vol. 72, no. 4, pp. 5290–5299, 2023.
- [22] F. Shahzad, T. R. Sheltami, and E. M. Shakhshuki, "Dv-maxhop: A fast and accurate range-free localization algorithm for anisotropic wireless networks," *IEEE Transactions on Mobile Computing*, vol. 16, no. 9, pp. 2494–2505, 2017.
- [23] Z. Cui, B. Sun, G. Wang, Y. Xue, and J. Chen, "A novel oriented cuckoo search algorithm to improve dv-hop performance for cyber-physical systems," *Journal of Parallel and Distributed Computing*, vol. 103, pp. 42–52, 2017.
- [24] L. Gui, F. Xiao, Y. Zhou, F. Shu, and T. Val, "Connectivity based dv-hop localization for internet of things," *IEEE Transactions on Vehicular Technology*, vol. 69, no. 8, pp. 8949–8958, 2020.
- [25] P. Wang, J. Huang, Z. Cui, L. Xie, and J. Chen, "A gaussian error correction multi-objective positioning model with nsga-ii," *Concurrency and Computation: Practice and Experience*, vol. 32, no. 5, p. e5464, 2020.

- [26] V. Kanwar and A. Kumar, "Multiobjective optimization-based dv-hop localization using nsga-ii algorithm for wireless sensor networks," *International Journal of Communication Systems*, vol. 33, no. 11, p. e4431, 2020.
- [27] A. Ouyang, Y. Lu, Y. Liu, M. Wu, and X. Peng, "An improved adaptive genetic algorithm based on dv-hop for locating nodes in wireless sensor networks," *Neurocomputing*, vol. 458, pp. 500–510, 2021.
- [28] Y. Jin, L. Zhou, L. Zhang, Z. Hu, and J. Han, "A novel range-free node localization method for wireless sensor networks," *IEEE Wireless Communications Letters*, vol. 11, no. 4, pp. 688–692, 2022.
- [29] J. Wang, L. Cheng, Y. Tu, and S. Gu, "A novel localization approach for irregular wireless sensor networks based on anchor segmentation," *IEEE Sensors Journal*, vol. 22, no. 7, pp. 7267–7276, 2022.
- [30] J. Liu, M. Liu, X. Du, P. S. Stanimirovi, and L. Jin, "An improved dv-hop algorithm for wireless sensor networks based on neural dynamics," *Neurocomputing*, vol. 491, pp. 172–185, 2022.
- [31] W. Jia, G. Qi, M. Liu, and J. Zhou, "A high accuracy localization algorithm with dv-hop and fruit fly optimization in anisotropic wireless networks," *Journal of King Saud University - Computer and Information Sciences*, vol. 34, no. 10, pp. 8102–8111, 2022.
- [32] Y. Cao and J. Xu, "Dv-hop-based localization algorithm using optimum anchor nodes subsets for wireless sensor network," *Ad Hoc Networks*, vol. 139, p. 103035, 2023.
- [33] G. Tan, H. Jiang, S. Zhang, Z. Yin, and A.-M. Kermarrec, "Connectivity-based and anchor-free localization in large-scale 2d/3d sensor networks," *ACM Transactions on Sensor Networks*, vol. 10, no. 1, dec 2013.
- [34] W. Cui, C. Wu, W. Meng, B. Li, Y. Zhang, and L. Xie, "Dynamic multidimensional scaling algorithm for 3-d mobile localization," *IEEE Transactions on Instrumentation and Measurement*, vol. 65, no. 12, pp. 2853–2865, 2016.
- [35] J. Fan, Y. Hu, T. H. Luan, and M. Dong, "Disloc: A convex partitioning based approach for distributed 3-d localization in wireless sensor networks," *IEEE Sensors Journal*, vol. 17, no. 24, pp. 8412–8423, 2017.
- [36] X. Liu, J. Yin, S. Zhang, B. Ding, S. Guo, and K. Wang, "Range-based localization for sparse 3-d sensor networks," *IEEE Internet of Things Journal*, vol. 6, no. 1, pp. 753–764, 2019.
- [37] X. Cai, P. Wang, L. Du, Z. Cui, W. Zhang, and J. Chen, "Multi-objective three-dimensional dv-hop localization algorithm with nsga-ii," *IEEE Sensors Journal*, vol. 19, no. 21, pp. 10 003–10 015, 2019.
- [38] V. Kanwar and A. Kumar, "Range free localization for three dimensional wireless sensor networks using multi objective particle swarm optimization," *Wireless Personal Communications*, vol. 117, no. 2, pp. 901–921, 2021.
- [39] D. K. Sah, T. N. Nguyen, M. Kandulna, K. Cengiz, and T. Amgoth, "3d localization and error minimization in underwater sensor networks," *ACM Transactions on Sensor Networks*, vol. 18, no. 3, 2022. [Online]. Available: <https://doi.org/10.1145/3460435>
- [40] H. Y. Abuaddous, G. Kaur, K. Jyoti, N. Mittal, S. Mahajan, A. K. Pandit, A. R. Alsoud, and L. Abualigah, "Repulsion-based grey wolf optimizer with improved exploration and exploitation capabilities to localize sensor nodes in 3d wireless sensor network," *Soft Computing*, vol. 27, no. 7, pp. 3869–3885, 2023.
- [41] M.-M. Cheng, J. Zhang, D.-G. Wang, W. Tan, and J. Yang, "A localization algorithm based on improved water flow optimizer and max-similarity path for 3-d heterogeneous wireless sensor networks," *IEEE Sensors Journal*, vol. 23, no. 12, pp. 13 774–13 788, 2023.
- [42] P. Wang, H. Li, and X. Cai, "3d many-objective dv-hop localization model with nsga3," *Soft Computing*, 2023.
- [43] K. Deb, A. Pratap, S. Agarwal, and T. Meyarivan, "A fast and elitist multiobjective genetic algorithm: Nsga-ii," *IEEE Transactions on Evolutionary Computation*, vol. 6, no. 2, pp. 182–197, 2002.